

PCCP

Accepted Manuscript



This is an *Accepted Manuscript*, which has been through the Royal Society of Chemistry peer review process and has been accepted for publication.

Accepted Manuscripts are published online shortly after acceptance, before technical editing, formatting and proof reading. Using this free service, authors can make their results available to the community, in citable form, before we publish the edited article. We will replace this *Accepted Manuscript* with the edited and formatted *Advance Article* as soon as it is available.

You can find more information about *Accepted Manuscripts* in the [Information for Authors](#).

Please note that technical editing may introduce minor changes to the text and/or graphics, which may alter content. The journal's standard [Terms & Conditions](#) and the [Ethical guidelines](#) still apply. In no event shall the Royal Society of Chemistry be held responsible for any errors or omissions in this *Accepted Manuscript* or any consequences arising from the use of any information it contains.

Modulating magnetic behavior of Fe(II)-MOF-74 by high electron affinity of the guest molecule

Sungmin Han,[†] Heejin Kim,^{†,‡} Jaehoon Kim,[†] and Yousung Jung^{†,}*

[†]Graduate School of Energy, Environment, Water and Sustainability (EEWS), Korea Advanced Institute of Science and Technology, Daejeon, 305-701, Republic of Korea

[‡]Analysis Research Division, Suncheon Center, Korea Basic Science Institute, Suncheon 540-742, Republic of Korea

Keywords : metal-organic framework, magnet, superexchange, first-principles

ABSTRACT

As a new class of magnetic materials, metal-organic framework (MOF) has received a significant attention due to its functionality and porosity that can provide diverse magnetic phenomena by utilizing the host-guest chemistry. For Fe-MOF-74, we here find using density functional calculations that the O₂ and C₂H₄ adsorptions respectively result in the ferromagnetic (FM) and antiferromagnetic (AFM) orderings along the 1D chain of hexagonal MOF framework, while their adsorption energies, pi-complexation, and the geometry changes are all similar upon binding. We reveal that this different magnetism behavior is attributed to the different electronic effects, where the adsorbed O₂ greatly withdraws a minor spin electron from the Fe centers. The latter significant back donation opens a new channel for superexchange interaction that can enhance the FM coupling between Fe centers. This prediction suggests a possibility for the conceptual usage of Fe-MOF-74 as a gas sensor based on its magnetic changes caused by the adsorbed gases. Furthermore, the suggested mechanism might be used to control the magnetic properties of MOFs using the guest molecules, although concrete strategies to enhance such magnetic interactions to be used in practical applications would require significant further investigations.

INTRODUCTION

Many metal-organic frameworks (MOFs) can have various magnetic properties due to the unpaired electrons in the metals that are periodically arranged. Unlike the other solid-state magnetic materials, MOFs provide the pores with high surface area that can interact with guest molecules. Thereby, one can anticipate that some MOFs can exhibit a guest-induced change of magnetism that is potentially useful for magnetic sensors, drug delivery, and magnetic separations.¹⁻⁶ Specifically, the spin crossover between low- and high-spin states,⁷⁻¹¹ transition between ferromagnetic (FM) and antiferromagnetic (AFM) orderings,¹²⁻¹⁵ and change in the critical ordering temperature (T_c)¹⁶⁻¹⁹ have been reported in MOF systems. The Fe-MOF-74, which is one of the most extensively studied MOFs for its gas handling applications as well as magnetic phenomena,²⁰⁻³¹ is also known to show these magnetic switching behaviors when interacting with guest molecules.

The Fe-MOF-74 is composed of one dimensional (1D) chains of the inorganic unit that are interconnected with each other by organic linkers in lateral direction (Figure 1). In each 1D chain, the Fe(II) atoms are connected through two bridge oxygen atoms, i.e., two Fe–O–Fe bonds that can be considered as superexchange interaction channels. Since such Fe–O–Fe bond angles are around 90°, the distance between nearest-neighbor (NN) Fe(II) atoms along the 1D chain is quite small (2.99 Å), also allowing a direct exchange interaction between Fe(II) atoms. As a result, the net sum of these direct- and super-exchange interactions yields a weak FM coupling (exchange coupling constant $J = 4.12 \text{ cm}^{-1}$) between Fe centers along the 1D chain, developing an intrachain FM ordering.²¹ To maintain the zero net spin overall, the interchain spins are then antiparallely aligned. Interestingly, however, when Fe-MOF-74 combines with olefin molecules, it was observed that its intrachain FM ordering turns into AFM ordering with negative coupling constants of $-1.1 - -3.9 \text{ cm}^{-1}$ depending on the type of olefins.²¹

Later, this magnetism transition of Fe-MOF-74 upon olefin adsorption was interpreted to be due to the guest-induced geometry change of the host framework.^{24, 25} That is, the adsorbed olefins increase the Fe–Fe distance and Fe–O–Fe angle that both strengthen the AFM coupling between Fe centers by diminishing direct exchange and enhancing superexchange interactions, respectively. To prove it, it was shown computationally that an expanded model host structure that is artificially distorted to accommodate C₂H₄ but without actually including the guest molecule possesses an intrachain AFM ordering even in the absence of the guest molecules. In other words, the electronic effects of the guest on the host magnetism was not direct, but was rather indirect through the structural alterations of the host framework upon binding.

While the above instance shows an importance of the geometry (ionic position), a detailed electron configuration should also be considered in general since the magnetism is a delicate result of the overlap between electrons in the end. In this work, we demonstrate that the direct electronic effects could indeed be important for the magnetism of Fe-MOF-74 using the triplet O₂ as a guest molecule. Here, in addition to the paramagnetic characteristic, the strong electron withdrawing nature of molecular O₂ can induce a significant perturbation in the electro-magnetic structure of host adsorbent. We note that, in fact, a partial oxidation of Fe center, i.e. partial migration of electrons from Fe(II) to O₂, was experimentally observed in the O₂ adsorbed Fe-MOF-74 system.^{20, 32} In spite of such an intriguing phenomenon, the electronic structures and the role of adsorbate O₂ in this system have not been studied for its magnetic properties.

In this paper, we first investigated the binding nature of O₂ on Fe-MOF-74; and further, we predict that this system exhibits a strong intrachain FM ordering at low temperature, despite the fact that its geometry is almost similar to that of the olefin adsorbed cases which showed the AFM ordering. We interpret this sharp contrast using the Goodenough–Kanamori–

Anderson (GKA) rules³³⁻³⁶ that the intrachain magnetism of O₂ adsorbed Fe-MOF-74 is due to the significant charge-transfer mediated superexchange interaction.

COMPUTATIONAL METHODS

Models. We denote the bare Fe-MOF-74, C₂H₄ adsorbed Fe-MOF-74, and O₂ adsorbed Fe-MOF-74 as the structure **1**, **2a**, and **3a**, respectively. The **2b** and **3b** denote the same structures as **2a** and **3a** but with the guest molecules (C₂H₄ or O₂) removed for analysis. The initial structures of **1**, **2a**, and **3a** were taken from the experimentally refined results.^{20, 21} In the case of **3a**, we used the low temperature structure (< 211 K), which has 1 molecule of O₂ per open Fe site.²⁰ We considered the O₂ molecules only at the first coordination sphere since the other O₂ molecules that are weakly bound via dispersion interaction (~10 kJ/mol) barely affect the host framework. We used supercells that contain 6 Fe atoms per each 1D chain to describe the intrachain magnetic ordering as suggested by Capena et al.³⁷

Calculation Details. The periodic density functional theory (DFT) calculations were performed based on the Vienna Ab-initio Simulation Package (VASP).³⁸ We used the RPBE exchange-correlation functional³⁹ with a dispersion correction of Grimme's D2.⁴⁰ We also used an effective U parameter of 1.0 eV for Fe atoms under the spherically averaged form.⁴¹ This value of $U = 1.0$ eV was chosen to reproduce the experimental measurements such as binding energy of guest molecules, magnetic coupling constants, and geometries, when used in conjunction with the RPBE functional augmented with the D2 correction. Therefore, All structures were fully optimized using RPBE+D2 functional with $U = 1.0$ eV until their remaining forces were less than 0.02 eV/Å. We adopted a plane wave basis set and the projector-augmented wave (PAW) method⁴² with an energy cut-off of 500 eV. The total

energy was sampled at $2 \times 2 \times 2$ Monkhorst–Pack k-point mesh in all calculations.⁴³ The Bader charge analysis was used to obtain the charge and magnetic moment values.⁴⁴ All crystal structures in this study were visualized using the VESTA program.⁴⁵

To compare with the intrachain magnetic coupling constants (J_{in}) from experimental measurements, we used the Heisenberg model to calculate J_{in} , i.e., $H = -2J_{\text{in}}\sum S_{\text{Fe1}}S_{\text{Fe2}}$, where $|S_{\text{Fe1}}| = |S_{\text{Fe2}}|$ are the calculated spin magnetic moment of Fe centers.^{33,37} We note that the next nearest-neighbor coupling (J_{NNN}),³⁷ single-ion anisotropy,²³ and interchain coupling are not considered here since their effects are secondary and much less influential in the intrachain coupling. We also assumed that all spin centers are either aligned in a parallel (FM) or antiparallel (AFM) manner.

RESULTS AND DISCUSSION

Table 1 summarizes the calculated preferred magnetic orderings and associated magnetic, energetic, and geometric parameters for the Fe-MOF-74 systems upon the gas (O_2 or C_2H_4) adsorption. Experimental coupling constants are also presented for comparison. Overall, excellent agreements between theory and experiments are found for all available experimental data; the calculated adsorption energies of O_2 and C_2H_4 are 41.8 and 46.2 kJ/mol, respectively, as compared with experiments (41 kJ/mol²⁰ and 45 kJ/mol²¹, respectively), and the calculated intrachain magnetic coupling constants (J_{in}) are also in good agreement with experiments for the bare MOF and C_2H_4 adsorbed cases.

For both C_2H_4 and O_2 adsorbed cases, the Fe-MOF-74 host framework with the adsorbed guest molecules removed, denoted as **2b** and **3b** structures, respectively, exhibit an AFM ordering along the 1D chain. Note that both structures **2b** and **3b** are compositionally identical to the structure **1**, bare Fe-MOF-74, but their different geometries result in a different magnetism due to the superexchange interactions through bridge oxygens.²⁵ To be

more specific, indicated in Table 1, the Fe–Fe distance for **1** (2.99 Å) is close enough to have the direct exchange interaction between the adjacent Fe centers, which leads to the FM ordering (see Ref. 25 for the direct exchange schemes).²⁵ In **2b** and **3b**, however, because of the increased Fe–Fe distances (3.25 Å for **2b** and 3.22 Å for **3b**), the Fe–O^{br}–Fe superexchange interaction dominantly affects the intrachain magnetic coupling and causes the AFM ordering. Furthermore, the increased Fe–O^{br}–Fe angles in **2b** and **3b** also strengthen the AFM coupling.²⁵

When the O₂ guest molecules exist, however, the electronic effect from the adsorbed O₂ turns the intrachain coupling back to FM for structure **3a** as in bare MOF. It can be compared with the C₂H₄ adsorbed case in which the additional electronic effect besides the geometric change does not alter the magnetic ordering (AFM) between structures **2a** and **2b**.

To understand this sharp difference between the O₂ and C₂H₄ adsorptions, we first investigated the electronic interaction between adsorbed O₂ and Fe-MOF-74 host framework. By defining *z*-axis to be the direction of open Fe site, each O₂ molecule approaches the host along the *z*-direction in a side-on manner as shown in Figure 1b. The calculated binding distance ($d_{\text{Fe-O}} = 2.17 \text{ \AA}$) and strength (41.8 kJ/mol) agree well with previous experiments (2.10 Å and 41 kJ/mol).²⁰

Figure 2a and 2b respectively show the density of states (DOS) before and after the adsorption of O₂ on Fe-MOF-74. Before the adsorption (Figure 2a), the highest occupied molecular orbital (HOMO) of free O₂ molecule is two degenerate antibonding orbitals, π^*_{px} and π^*_{pz} , each of these antibonding orbitals singly occupied by one unpaired electron. Meanwhile, the host structure **3b** has a localized minor spin electron that mainly occupies the d_{yz} orbital of Fe(II) atom, denoted as Fe– d_{yz} , at the HOMO level. Hereafter we define the down spin electrons as minor. After the adsorption (Figure 2b), it is clear that the

directionally well-matched π^*_{pz} orbital of O_2 , denoted as $O_2-\pi^*_{pz}$, can interact with the $Fe-d_{yz}$ as marked with (i) and (ii).

For adsorbed O_2 at the energy level of (i) in Figure 2b, the down spin electron in $Fe-d_{yz}$ (HOMO of host) partially transfers to the singly occupied $O_2-\pi^*_{pz}$ orbital due to a high electron affinity of O_2 , resulting in the oxidation of Fe center from 2+ to 2~3+ (intermediate state), consistent with experiments.²⁰ Specifically, in Mossbauer measurements, Fe in the present O_2 adsorbed Fe-MOF-74 showed the oxidation state to be halfway between Fe(II) and Fe(III). In the neutron power diffraction data, the O–O distance in the adsorbed state (1.25 Å) was also between isolated O_2 molecule (1.21 Å) and O^{2-} superoxide unit (1.28 Å), indicating the partial charge transfer from Fe to O_2 .²⁰ This significant charge transfer of the down spin electron is also evident in our calculations from the decreased magnetic moment of adsorbed oxygen (from 1.0 to 0.76) and increased magnetic moment of the host Fe (from 3.66 to 3.93) as shown in Table 1, as well as the increased charge in the 2p orbitals of O in O_2 (from 6.00 to 6.18). This net charge transfer from the guest to Fe does not dominantly occur in the C_2H_4 adsorbed case, supported by no apparent change in magnetic moments in Fe and the decreased charge in the 2p orbitals of C in C_2H_4 (from 4.00 to 3.85) mainly by the forward donation. Therefore, the back donation from $Fe-d_{yz}$ to $O_2-\pi^*_{pz}$ makes a noticeable backbonding (Figure 2c) as in the olefin adsorption cases²⁴ but much more significantly in the present case due to the high electron affinity of O_2 . Its schematic description is also shown in Figure 3a. In contrast, at the energy level of (ii), the similar orbital mixing with the Fe up spin electrons is not observed (Figure 2d) since the up spin state of $O_2-\pi^*_{pz}$ orbital is already occupied; thereby only a weak exchange interaction is expected to occur between the up spin electrons of $O_2-\pi^*_{pz}$ and $Fe-d_{yz}$.

As a brief conclusion so far, thus, when O_2 molecules are adsorbed on Fe-MOF-74, electronic interactions are most significant between the singly occupied $O_2-\pi^*_{pz}$ and the

HOMO of Fe-MOF-74 (Fe- d_{yz}), suggesting that the d_{yz} orbital of Fe(II/III) atom may be responsible for the observed magnetic transition from AFM in **3b** to FM in **3a** after considering electronic interactions with the guest.

Based on this electronic structure analysis, we now explain the magnetic behavior of Fe-MOF-74 upon O_2 adsorption summarized in Table 1 using the GKA rules for the superexchange interaction.³³⁻³⁶ In GKA rules, the magnetic coupling is mediated through the pair of p electrons of the bridging oxygen atom (O^{br}). As shown in Figure 3b, one electron in one of the p orbitals of O^{br} transfers to the Fe center at one side (Fe1), with the remaining p electrons of O^{br} interacting with the Fe center at the other side (Fe2). For the former Fe1- O^{br} electron transfer, both σ - and π -types (depending on the symmetry of orbital alignment) are available, where the σ -charge transfer is dominant over the π -charge transfer.^{33, 34} The O^{br} -Fe2 interaction can then be either an exchange interaction (EX) or charge transfer (CT) depending on the orbital symmetry, making the Fe1-Fe2 coupling either FM or AFM, respectively. When the mediating p orbital of O^{br} is nearly orthogonal to all the valence orbitals of Fe2 center (dotted arrow in Figure 3), there is only an exchange interaction that prefers the parallel spin alignment, which leads to the FM coupling between Fe1 and Fe2. On the other hands, if the nonorthogonal overlap dominates over the exchange (solid arrow in Figure 3), the spin interactions would result in the AFM coupling between two Fe centers. For example, for the $Fe^{2+}-O-Fe^{2+}$ case of the present interest, these GKA rules suggest that a strong AFM coupling is general for the bond angle of 180° , while for the bond angle of 90° the type of magnetic coupling is not definitive or usually weakly FM.^{33, 34} Similar arguments for exchange vs. superexchange interactions lead to ferromagnetic vs. antiferromagnetic coupling in isolated molecules including Fe centers.⁴⁶

Following these GKA rules, for the bare Fe-MOF-74 of structure **1** that has a relatively short Fe-Fe distance (2.99 Å) and Fe-O-Fe angle of around 90° , all aforementioned

interactions, including the direct exchange, cooperatively play to result in a weak FM with a coupling constant of 4.12 cm^{-1} , as indeed observed experimentally²¹ and theoretically²⁵. In structure **3b**, i.e., bare MOF but its geometry distorted to accommodate O_2 adsorption, however, geometric distortions such as increased Fe–Fe distance and Fe–O–Fe angle enhance the relative strength of the AFM component (Table 1), yielding the intrachain AFM ordering favored in the framework (**3b**). However, when O_2 molecules physically exist to interact with the open Fe sites electronically, i.e., in structure **3a**, this intrachain AFM ordering interestingly turns back to the FM. We show below that this electronic effect is due to the electron withdrawal of O_2 from the transition metals.

An important feature of Fe-MOF-74, which has a high spin configuration of d_6 (Fe^{2+}), is that one down spin electron is strongly localized in d_{yz} orbital since it is spatially less crowded, i.e., more stable, than the other d orbitals. Thus, the d_{yz} orbital is a closed-shell in Fe-MOF-74 when no guest molecules are present. As shown in previous paragraphs, however, adsorbed O_2 molecules extract partially this localized down spin electron from the Fe center, enabling the resulting unpaired electron in d_{yz} orbital to participate in the superexchange interaction. In other words, the high electron affinity of adsorbed O_2 molecules “activates” the d_{yz} orbital to be an open-shell for possible superexchange interactions.

Figure 4 is a schematic representation of the superexchange interaction through the possible σ -charge transfers, which are dominant over π -charge transfers. The main structure is derived from Figure 1b with an assumption that the Fe–O–Fe angles are 90° despite a small deviation from an ideal orthogonal geometry. In Figure 4, we set the unpaired 3d electrons of two neighboring Fe atoms, Fe1 and Fe3, to be aligned upward. Then, the spin state of Fe2 in the middle determines whether the magnetic coupling is FM or AFM: if the unpaired

electrons in the Fe2 prefer to be aligned upward, the magnetic coupling along the chain will be FM, and similarly for AFM.

Since all the up spin states of Fe1 and Fe3 atoms are occupied in Fe-MOF-74, there are σ -type down spin electron transfers from each p_σ orbital of O^{br} to the e_g orbitals ($d_{x^2-y^2}$ and d_{z^2}) of Fe1 and Fe3 atoms (solid arrows in Figure 4). Then, the remaining up spin electrons in each p_σ orbital interact with the d_{yz} orbital of Fe2 center (dashed arrows in Figure 4). The latter interaction is an exchange that stabilizes the parallel spin alignment since all the p_σ orbitals are nearly orthogonal to the d_{yz} orbital of the Fe2 (with weak orbital mixing), contributing to develop the FM coupling along the Fe1–Fe2–Fe3 chain. (See SI for the supporting approximate relative degree of orbital overlaps between the p_σ orbitals of O^{br} and Fe2– d_{yz} vs. Fe1– or Fe3– e_g). Therefore, the adsorbed O_2 molecules bring the FM ordering along the intrachain by activating the d_{yz} orbitals of Fe centers.

CONCLUSIONS

We showed that high electron affinity of a gas molecule such as O_2 can modulate the magnetic behavior of the MOF framework by withdrawing a minor spin electron from the Fe centers in Fe-MOF-74, a phenomenon not seen for the adsorption of C_2H_4 on the same MOF. In the O_2 adsorption, a back donation of electrons arises from the HOMO of Fe-MOF-74 (d_{yz} orbital) to the singly occupied MO of O_2 molecules, leading to the partial oxidation of Fe center. The latter charge transfer then results in a strong FM coupling between Fe centers along the 1D chain of Fe-MOF-74 by generating additional unpaired electrons in the d_{yz} orbitals of Fe, which were closed-shell otherwise before the O_2 adsorption. This unpaired electron in d_{yz} orbitals can then participate in superexchange interactions, which according to the GKA rules, lead to the intrachain FM ordering in Fe-MOF-74. We are currently studying whether other electron withdrawing or electron rich guest molecules can also modify the

magnetic exchange interactions as suggested here, but this demonstration does suggest a new way to modulate the magnetic ordering of MOFs using the electron affinity of guest molecules, helping to develop the magnetic materials and sensors. In particular, significant further investigations for the concrete strategies to enhance such magnetic interactions to the extent to be used in practical applications would be required to make the proposed concept in real applications.

Corresponding Author

*E-mail: ysjn@kaist.ac.kr

ACKNOWLEDGMENT

We acknowledge the financial support by grant from Korea CCS R&D Center (NRF-2014M1A8A1049252) funded by National Research Foundation of Korea (NRF). A generous computing time from KISTI is also gratefully acknowledged.

REFERENCES

1. P. Dechambenoit and J. R. Long, *Chemical Society Reviews* 2011, **40**, 3249-3265.
2. B. V. Harbuzaru, A. Corma, F. Rey, P. Atienzar, J. L. Jorda, H. Garcia, D. Ananias, L. D. Carlos and J. Rocha, *Angewandte Chemie (International ed. in English)*, 2008, **47**, 1080-1083.
3. S.-H. Huo and X.-P. Yan, *Analyst*, 2012, **137**, 3445-3451.
4. F. Ke, Y.-P. Yuan, L.-G. Qiu, Y.-H. Shen, A.-J. Xie, J.-F. Zhu, X.-Y. Tian and L.-D. Zhang, *Journal of Materials Chemistry*, 2011, **21**, 3843-3848.

5. M. R. Lohe, K. Gedrich, T. Freudenberg, E. Kockrick, T. Dellmann and S. Kaskel, *Chemical Communications* 2011, **47**, 3075-3077.
6. M. Vallet-Regi, F. Balas and D. Arcos, *Angewandte Chemie (International ed. in English)*, 2007, **46**, 7548-7558.
7. G. J. Halder, K. W. Chapman, S. M. Neville, B. Moubaraki, K. S. Murray, J. F. Letard and C. J. Kepert, *Journal of the American Chemical Society* 2008, **130**, 17552-17562.
8. M. Ohba, K. Yoneda, G. Agusti, M. C. Munoz, A. B. Gaspar, J. A. Real, M. Yamasaki, H. Ando, Y. Nakao, S. Sakaki and S. Kitagawa, *Angewandte Chemie (International ed. in English)*, 2009, **48**, 4767-4771.
9. G. J. Halder, C. J. Kepert, B. Moubaraki, K. S. Murray and J. D. Cashion, *Science*, 2002, **298**, 1762-1765.
10. R. Ohtani, M. Arai, H. Ohba, A. Hori, M. Takata, S. Kitagawa and M. Ohba, *European Journal of Inorganic Chemistry*, 2013, **2013**, 738-744.
11. E. Coronado, M. Gimenez-Marques, G. Minguez Espallargas, F. Rey and I. J. Vitorica-Yrezabal, *Journal of the American Chemical Society* 2013, **135**, 15986-15989.
12. S. Ohkoshi, K. Arai, Y. Sato and K. Hashimoto, *Nature Materials*, 2004, **3**, 857-861.
13. N. Motokawa, S. Matsunaga, S. Takaishi, H. Miyasaka, M. Yamashita and K. R. Dunbar, *Journal of the American Chemical Society* 2010, **132**, 11943-11951.
14. M. Kurmoo, H. Kumagai, K. W. Chapman and C. J. Kepert, *Chemical Communications* 2005, 3012-3014.
15. M. Wriedt, A. A. Yakovenko, G. J. Halder, A. V. Prosvirin, K. R. Dunbar and H. C. Zhou, *Journal of the American Chemical Society* 2013, **135**, 4040-4050.
16. S. Ohkoshi, Y. Tsunobuchi, H. Takahashi, T. Hozumi, M. Shiro and K. Hashimoto, *Journal of the American Chemical Society* 2007, **129**, 3084-3085.

17. D. Pinkowicz, R. Podgajny, B. Gawel, W. Nitek, W. Lasocha, M. Oszajca, M. Czapla, M. Makarewicz, M. Balanda and B. Sieklucka, *Angewandte Chemie (International ed. in English)*, 2011, **50**, 3973-3977.
18. J. A. Navarro, E. Barea, A. Rodriguez-Dieguez, J. M. Salas, C. O. Ania, J. B. Parra, N. Masciocchi, S. Galli and A. Sironi, *Journal of the American Chemical Society* 2008, **130**, 3978-3984.
19. W. Kaneko, M. Ohba and S. Kitagawa, *Journal of the American Chemical Society* 2007, **129**, 13706-13712.
20. E. D. Bloch, L. J. Murray, W. L. Queen, S. Chavan, S. N. Maximoff, J. P. Bigi, R. Krishna, V. K. Peterson, F. Grandjean, G. J. Long, B. Smit, S. Bordiga, C. M. Brown and J. R. Long, *Journal of the American Chemical Society* 2011, **133**, 14814-14822.
21. E. D. Bloch, W. L. Queen, R. Krishna, J. M. Zadrozny, C. M. Brown and J. R. Long, *Science*, 2012, **335**, 1606-1610.
22. P. Verma, X. Xu and D. G. Truhlar, *The Journal of Physical Chemistry C*, 2013, **117**, 12648-12660.
23. R. Maurice, P. Verma, J. M. Zadrozny, S. Luo, J. Borycz, J. R. Long, D. G. Truhlar and L. Gagliardi, *Inorganic chemistry*, 2013.
24. H. Kim, J. Park and Y. Jung, *Physical Chemistry Chemical Physics* 2013, **15**, 19644-19650.
25. J. Park, H. Kim and Y. Jung, *The Journal of Physical Chemistry Letters*, 2013, **4**, 2530-2534.
26. S. Geier, J. a. Mason, E. Bloch, W. Queen, M. Hudson, C. M. Brown and J. R. Long, *Chemical Science*, 2013, **4**, 2054-2061.
27. Y. He, R. Krishna and B. Chen, *Energy & Environmental Science*, 2012, **5**, 9107-9120.

28. Q. Zhang, B. Li and L. Chen, *Inorganic Chemistry*, 2013, **52**, 9356-9362.
29. H. Kim and Y. Jung, *The Journal of Physical Chemistry Letters*, 2014, **5**, 440-446.
30. J. Borycz, L.-c. Lin, E. D. Bloch, J. Kim, A. L. Dzuba, D. Semrouni, K. Lee, B. Smit and L. Gagliardi, *The Journal of Physical Chemistry C*, 2014, **118**, 12230-12240.
31. U. Bo, B. Barth, C. Paula, A. Kuhnt, W. Schwieger, A. Mundstock, J. Caro and M. Hartmann, *Langmuir*, 2013, **29**, 8592-8600.
32. S. Shimomura, M. Higuchi, R. Matsuda, K. Yoneda, Y. Hijikata, Y. Kubota, Y. Mita, J. Kim, M. Takata and S. Kitagawa, *Nature Chemistry*, 2010, **2**, 633-637.
33. J. B. Goodenough, *Magnetism and the Chemical Bond*, John Wiley & Sons, INC.: New York, 1963.
34. J. Kanamori, *Journal of Physics and Chemistry of Solids*, 1959, **10**, 87-98.
35. P. W. Anderson, *Physical Review*, 1950, **79**, 350-356.
36. P. W. Anderson, *Physical Review*, 1959, **115**, 2-13.
37. P. Canepa, Y. Chabal and T. Thonhauser, *Physical Review B*, 2013, **87**, 094407.
38. G. Kresse and J. Furthmüller, *Computational Materials Science*, 1996, **6**, 15-50.
39. B. Hammer, L. Hansen and J. Nørskov, *Physical Review B*, 1999, **59**, 7413-7421.
40. S. Grimme, *Journal of Computational Chemistry*, 2006, **27**, 1787-1799.
41. S. L. Dudarev, G. A. Botton, S. Y. Savrasov, C. J. Humphreys and A. P. Sutton, *Physical Review B*, 1998, **57**, 1505-1509.
42. P. E. Blöchl, *Physical Review B*, 1994, **50**, 17953-17979.
43. H. J. Monkhorst and J. D. Pack, *Physical Review B*, 1976, **13**, 5188-5192.
44. W. Tang, E. Sanville and G. Henkelman, *Journal of Physics: Condensed Matter* 2009, **21**, 084204.
45. K. Momma and F. Izumi, *Journal of Applied Crystallography*, 2008, **41**, 653-658.

46. L. Fohlmeister, K. R. Vignesh, F. Winter, B. Moubaraki, G. Rajaraman, R. Pottgen, K. S. Murray and C. Jones, *Dalton Transactions*, 2015, **44**, 1700-1708.

Table 1. The preferred magnetic orderings and associated magnetic, energetic, and geometric parameters upon O₂ and C₂H₄ adsorptions, compared with experiments

Structure of Fe-MOF-74	No.	Intrachain ordering	Coupling constant (J_{in} , cm ⁻¹)		Fe-Fe (Å)	Fe-O-Fe (°)	Mag. mom	Binding Energy (kJ/mol)	
			This work	Exp				This work	Exp
bare	1	FM	2.11	4.12	2.99	92.0, 89.9	3.66		
C ₂ H ₄ adsorbed	2a	AFM	-5.42	-3.9	3.25	104.0, 92.3	3.66	46.2	45
C ₂ H ₄ adsorbed frame	2b	AFM	-3.36		3.25	104.0, 92.3	3.66		
O ₂ adsorbed	3a	FM	24.4		3.22	103.7, 93.5	3.93	41.8	41
O ₂ adsorbed frame	3b	AFM	-15.1		3.22	103.7, 93.5	3.66		

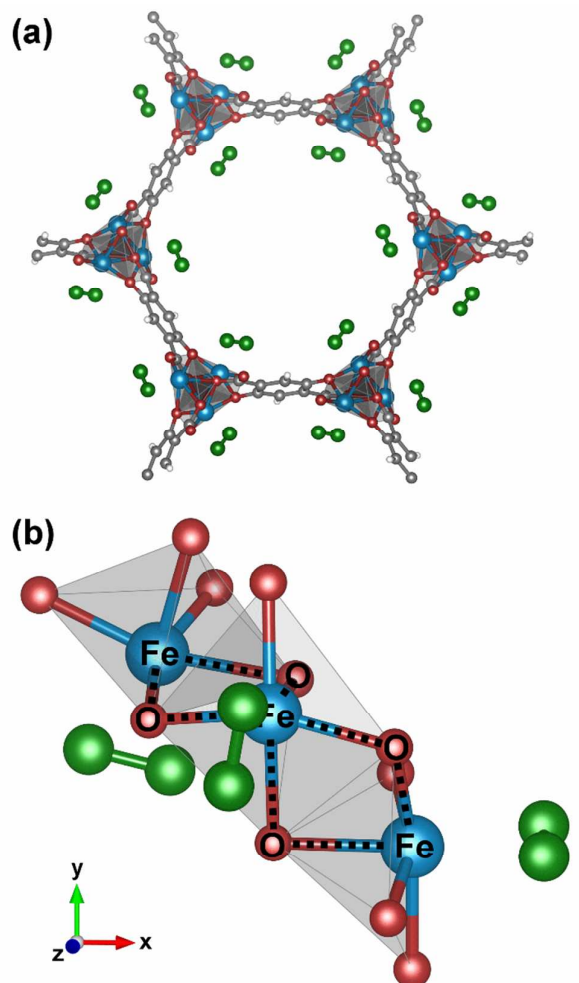


Figure 1. (a) The local structure of O_2 adsorbed Fe-MOF-74. (b) Fe atoms are interconnected with each other through two bridge O atoms along the 1D chain, denoted as black dotted lines. Blue, grey, and white are Fe, C, and H, respectively. Red and green are bridge O and adsorbed O_2 , respectively.

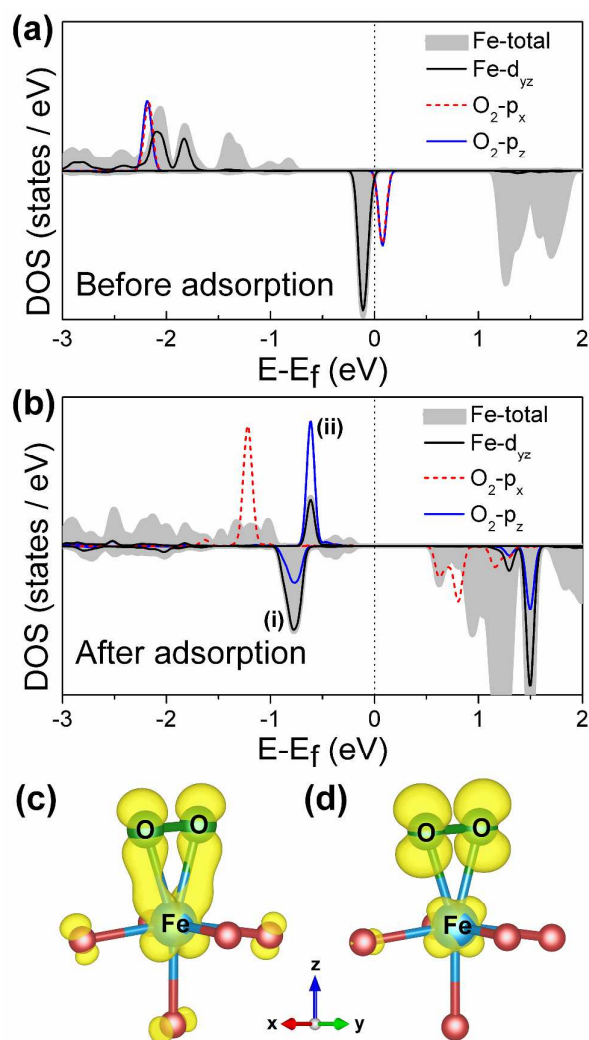


Figure 2. The density of states (DOS) for the O₂ + Fe-MOF-74 systems (a) before and (b) after the O₂ adsorption. See Table 1 for calculated binding energies and geometries. The electron density isosurfaces (orbital plot at isosurface level of 0.007) for energy level (i) and (ii) in Figure 2b are drawn in (c) and (d), respectively. The orbital plotted in (c) shows a backbonding, while that in (d) shows a nonbonding.

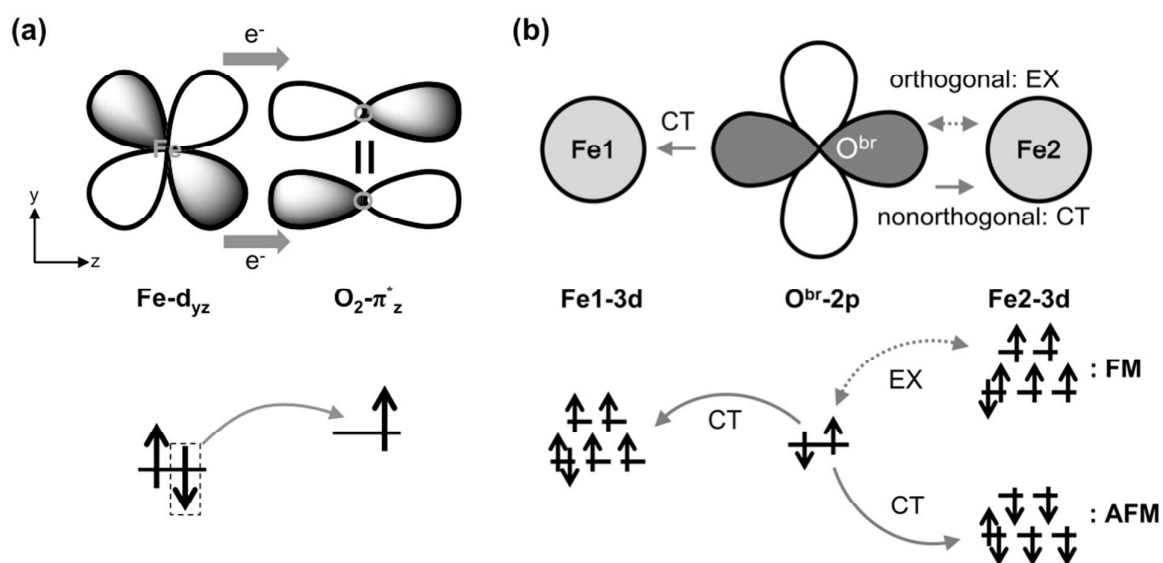


Figure 3. Schemes for (a) π backbonding between Fe-d_{yz} and $\text{O}_2-\pi_z^*$ and (b) superexchange interaction between Fe1 and Fe2 through the bridge oxygen (O^{br}) following the Goodenough–Kanamori–Anderson (GKA) rule.

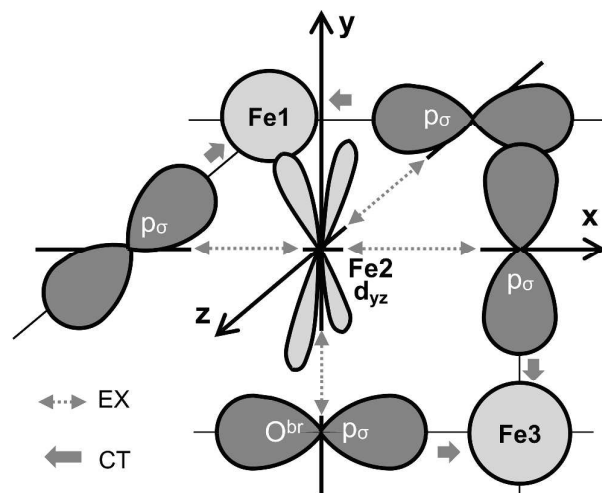
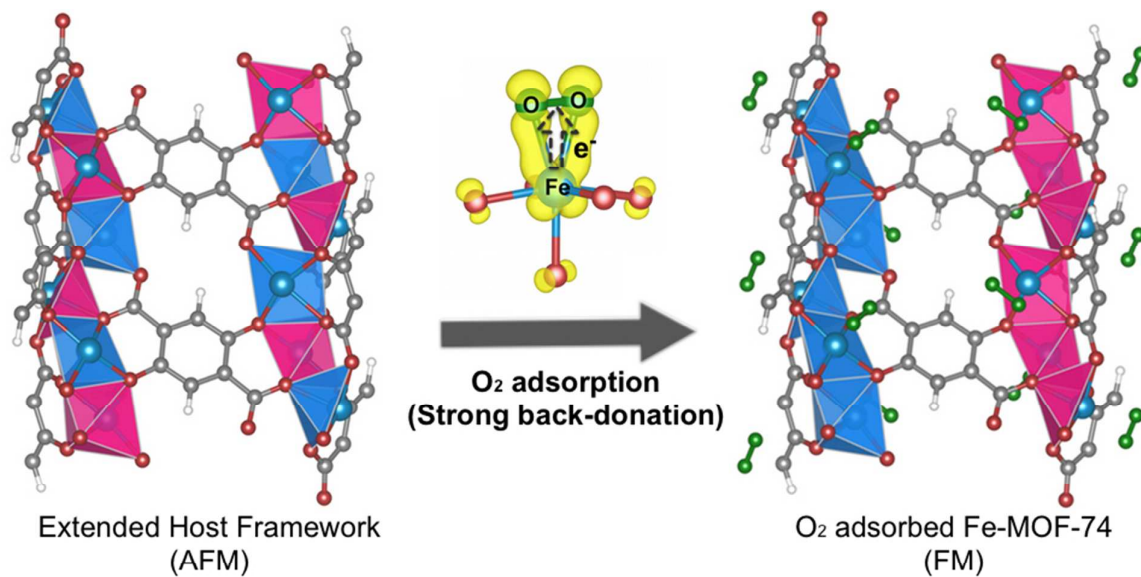


Figure 4. The contribution of d_{yz} orbital that has partial unpaired electron transferred from O_2 , to the superexchange interaction between Fe atoms along the 1D chain. See also Fig 3.

TOC



Intrachain magnetic coupling of Fe-MOF-74